2021

Development of Dynamic Modeling Framework Using Convolution Neuron Network for Variable Refrigerant Flow Systems

Hanlong Wan
University of Maryland

Tao Cao
University of Maryland, taocao@umd.edu

Yunho Hwang
University of Maryland

Saikee Oh
LG Electronics

Development of Dynamic Modeling Framework Using Convolution Neuron Network for Variable Refrigerant Flow Systems

Hanlong Wan[1], Tao Cao[1], Yunho Hwang[1]*, Simon Chin [2]

[1] 4164 Glenn Martin Hall Bldg., Center for Environmental Energy Engineering
Department of Mechanical Engineering, University of Maryland,
College Park, MD., 20742, United States

[2] Air Solution R&D Laboratory, LG Electronics, Seoul, Republic of Korea

*Corresponding author: 301-405-5247, yhhwang@umd.edu

ABSTRACT

Modeling the air conditioning system provides an excellent tool for system design, control, operation, and fault diagnosis. Such models were developed as either steady-state and transient models or knowledge-based and physics-based models. Most of the current studies mainly concentrated on physics-based models or steady-state models. Knowledge-based dynamic models were rarely discussed. In this paper, a knowledge-based dynamic model using a Convolutional Neural Network was developed for the air conditioning system. Instead of using operating parameters at a time point, we used the numbers in a time window as input data. We conducted a case study of the variable refrigerant flow system with field tests in an office building to validate this approach. It was found that the new method has a better accuracy within 2% deviation and a faster simulation speed in less than 1 second than the traditional physics-based model. The proposed method, which does not have a convergence problem, is user-friendly for non-experts. This approach also provides a way for existing systems to adjust operation parameters and detect faults. Future work can be making the current model more robust and reliable. In addition, how to combine the strengths of the knowledge-based method and physics-based methods needs to be further studied.

Keywords: Knowledge-based Dynamic Model, Convolutional Neural Network, Variable Refrigerant Flow System

1. INTRODUCTION

The term “variable refrigerant volume system” was first introduced in 1982 and is also known as the Variable Refrigerant Flow (VRF) system nowadays (Thornton and Wagner, 2012). Since the 1980s, VRF systems have been widely used in Japan: 50% of midsize office buildings up to 6,500 m^2 and 33% of large commercial buildings more than 6,500 m^2 (Goetzler, 2007). VRF systems have been introduced to the US around 2002 and are widely used in commercial and office buildings (Kwon et al., 2014). The VRF system typically consists of a variable speed compressor, an outdoor unit (OU), and multiple indoor units (IUs). The mass flow rate of each IU is controlled by the electronic expansion valve (EEV). This simple VRF system is also called the Heat Pump VRF (HPVRF) system (Kwon et al., 2014). VRF system has many advantages (Kwon et al., 2014). First, the system is flexible to operate as each IU can be controlled independently. In particular, the system with a variable speed compressor can easily match its cooling capacity to thermal loads at different indoor and ambient conditions. The VRF system is energy efficient as it does not lose energy through ductwork like conventional ducted unitary air conditioning systems. Since energy efficiency is an important characteristic of VRF systems, how to analyze the performance of a VRF system is a curtal task. Field tests and modeling works are vital tools to analyze the VRF system's performance (Wan et al., 2020b). Engaging readers on the field test could read the references (Kwon et al., 2014; Lin et al., 2014; Wan et al., 2019). Two modeling methods for VRF systems are physics-based and data-driven methods. The physics-based methods are white-box methods using physics-based correlations or equations to represent the VRF system's components, like the efficiency-based compressor model. The data-driven method is also known as the knowledge-based method. It was seldom used previously due to high computational cost and algorithm complicity.

Nevertheless, artificial intelligence technologies are widely used in almost every field nowadays. Machine learning is a method of data analysis that automates analytical model building (Nasrabadi, 2007). The number of studies using machine learning for VRF systems has been increasing in the recent five years. Various machine learning algorithms have been adopted. A summary is made here, and interested readers can read the references for each algorithm's details. Shi et al. (2017) combined Bayesian neural network with ReliefF classifier to detect low refrigerant charge. This combination method had a better performance than adopting each algorithm individually. Sun et al. (2016) proposed a new approach based on support vector machines (SVM), which resulted in a decrease in estimation error by 2.1%. Li et al. (2016c) found that the various virtual refrigerant charge sensors combined with the nonlinear SVR could reduce the estimation error to 5.5%. Liu et al. (2016, 2017) developed an index-weighted moving average method based on principal component analysis (PCA) to detect the refrigerant charge. Yu et al. (2018) proposed a VRF charge fault method based on expert modification C5.0 decision tree, and the overall accuracy could be improved by 4%. Based on the literature review, all the machine learning-based methods concentrated on steady-state or quasi-steady-state. In the previous study, dynamic modeling work for VRF systems using machine learning was seldom considered. The main challenge is that there is a gap between the simulation result and the real experiment result. The black box model using machine learning always uses frequency and EEV opening degree as the inputs. However, when the controller increased the compressor frequency and EEV opening degrees for the system setup period, the mass flow rate through the system would need time to rise. This time is usually 1 minute, according to our previous work (Wan et al., 2020a). Thus, if we only used the frequency and opening degree at the current time to predict the current mass flow rate, it would be somehow impossible. In this study, we developed a Convolutional Neural Network (CNN)-based dynamic modeling to predict the mass flow rate of the VRF system. We considered the parameters (like the frequency) at the current time and the present time of the parameters in the past few seconds.

2. METHODOLOGIES

2.1 Field Test Setting

We conducted a field test in a campus office building in College Park, Maryland, US. The installed ductless system had seven indoor units and one outdoor unit. The test time period was from June 2019 to August 2019. Pressure sensors were installed to measure the suction and discharge pressures of the compressor. The compressor frequency and the EEV opening degrees were directly read from the system's control software. Thermocouples were used for the temperature measurement. The accuracy of the instruments could be found in Table 1. The mass flow rate was measured by a mass flow meter. The data sampling time was 2 seconds. The nominal heating capacity of this system was 23.7 kW. The refrigerant of the system was R-410A. Our mass flow rate meter was installed on the liquid line. The mass flow rate was measured at the outlet of the condenser.

Table 1: Parameters of Measurement Instruments

Measurement	Range	Accuracy
T-type thermocouples	-200~350 °C	± 0.5 K
Pressure transducer (high-pressure side)	0~6,770 kPa	± 6.34 kPa
Pressure transducer (low-pressure side)	0~3,339 kPa	± 4.21 kPa
Coriolis mass flow meter	3~457.5 g/s	± 0.9 g/s

2.2 Data Processing

To simplify the case, we only considered the situation in which only one indoor unit was used. EEV opening degree, compressor suction pressure, compressor discharge pressure, condenser outlet temperature, condenser outlet density, evaporator inlet temperature, and compressor frequency were used as the input parameters. The outlet parameter was the mass flow rate through the system. The input data also had another dimension, which was the time. We considered 40 test data points for 80 seconds in this study. Each input data slot was an 8-by-40 matrix. The x-dimension was the

eight parameters we studied. The y-dimension was the time. An example is shown in Figure 1. It was an image generated by MATLAB. The inputs of the CNN model were consisted by a series of figures like Figure 1. Columns from left to right meanns EEV opening degree, condenser outlet temperature, compressor discharge pressure, evaporator inlet temperature, compressor suction pressure, subcooling of the condenser, condenser outlet density, and compressor frequency, respectively. There are 40 rows. The first row is the time 80 s ago. The last row is the current time. All the values were normalized to 0-1. Figure 1 was a greyscale photo from the normalized matrix. This example was in a quasi-steady state. Thus, the top side color is very closed to the downside color.

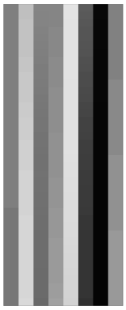

Figure 1: Input Example

2.3 CNN Model Setup

We had a set of images, as shown in the example. We also had a matching value for each photo, which was the mass flow rate and the output of our model. CNN was a standard method for image recognition. We used the 'trainNetwork' toolbox in MATLAB to build the CNN model. In our model, we set 6 hidden layers. Among 57,456 input data images, 30,000 were used as the training data set, 10,000 were used as the testing data set, and the remaining photos were used as the validation data set. The parameters of the model setting are listed in Table 2 (ReLU means Rectified Linear Unit, and the following list is in a set format used in the MATLAB toolbox).

Table 2 Parameters of model setting

No.	Layer	Note
1	Image Input	12x6x1 images with 'zerocenter' normalization
2	Convolution	8 3x3 convolutions with stride [1 1] and padding 'same'
3	Batch Normalization	-
4	ReLU	-
5	Average Pooling	2x2 average pooling with stride [2 2] and padding [0 0 0 0]
6	Convolution	16 3x3 convolutions with stride [1 1] and padding 'same'
7	Batch Normalization	-
8	ReLU	-
9	Average Pooling	2x2 average pooling with stride [2 2] and padding [0 0 0 0]
10	Convolution	32 2x2 convolutions with stride [1 1] and padding 'same'
11	Batch Normalization	-
12	ReLU	-
13	Convolution	32 2x2 convolutions with stride [1 1] and padding 'same'
14	Batch Normalization	
15	ReLU	
16	Dropout	20% dropout
17	Fully Connected	1 fully connected layer
18	Regression Output	Mean-Squared-Error

3. RESULTS AND DISSCUSIONS

3.1 Field Tests

Figure 2 shows the startup period of the VRF system when only one indoor unit was working. This test data was generated on July 11th at 9:16 am. The x-axis in all subfigures is the time. This last for 500 seconds, which also means that there are 250 data points in each subfigure. The first subfigure shows the condensing pressure and evaporating pressure. The condensing pressure increased at first, then decreased, and then increased again to a constant value. The evaporating pressure decreased and then kept at a constant value. This was due to the high pressure being controlled by the frequency of the compressor. As we could see in the second subfigure, the compressor frequency also increased at first, then decreased, and then increased again. The third subfigure shows the EEV opening degree of the target IU. The trending for that was similar to the high pressure and the compressor frequency. In this example, the time period was 500 seconds. At the end of this period, we could find that the system went into a quasi-steady state. In this figure, the pressure change and mass flow rate change had some delay as compared with the control parameters like compressor frequency and EEV opening degree. This delay is due to the system's control needing some time to reflect the users' control and operation. The main reason could be the thermal mass of the refrigerant in the heat exchangers.

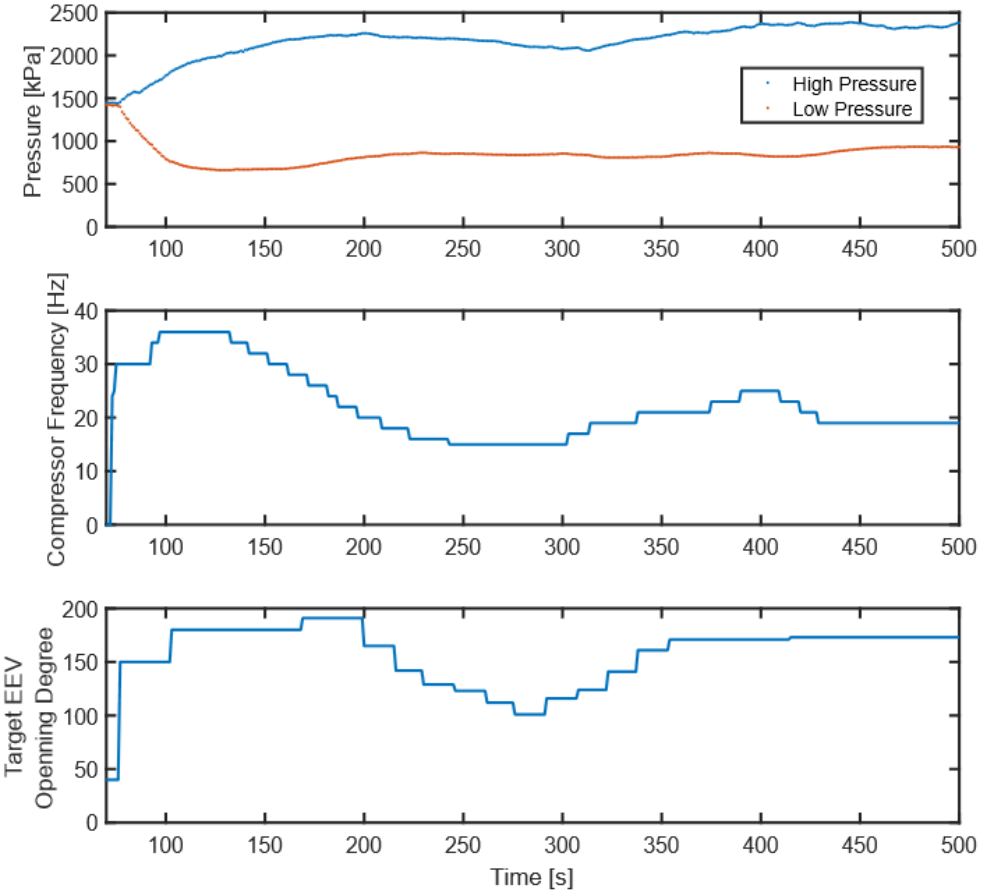

Figure 2: VRF system startup

3.2 Compressor Performance Map

We used the compressor performance map from the manufacturer to predict the system's mass flow rate and compared the result with our experiment data. The compressor performance map used was a 20-coefficients compressor map. Eq.1. shows the formulate.

$$\dot{m} = f(F, T_{dis}, T_{suc}) = M_1 + M_2 T_{dis} + M_3 T_{suc} + M_4 F + M_5 T_{dis} T_{suc} + \cdots + M_{20} T_{suc}^3 \quad (1)$$

In eq.1, M is the correlation factor. Tdis and Tsuc are measured by thermocouples. The unit of the temperatures is K. F is the frequency of the compressor, which was directly obtained from the control software.

This method has been widely used to evaluate the compressor mass flow rate for VRF systems. This method is also knowledge-based since no physics rules are used in this approach. This method could only be used for steady-state data or quasi-steady-state data. Our following results also proved this. Figure 3 shows the experiment value and predicted value from the compressor performance map. This 500-second period was the same as we showed in Figure 2. The experiment mass flow rate trend is following the compressor frequency trend and the EEV opening pulse trend. The mass flow rate increased sharply at first, then decreased, increased, and kept at a constant value. Figure 3 shows the mass flow rate measured at the liquid line and the mass flow rate predicted by the compressor performance map. For those time period when the mass flow rate varied a lot, the differnence is evident between the experimental and predicted values.

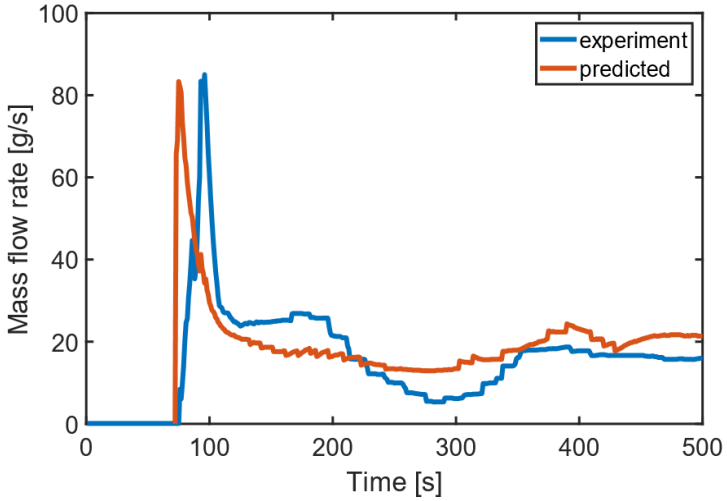

Figure 3: Mass Flow Rate Comparisons (Compressor Map vs. Experiment)

3.3 CNN Modeling Prediction

We applied the CNN-based modeling method as introduced in the methodology part to predict the mass flow rate at the same time. Figure 4 shows the result. As shown in Figure 4, the CNN-based model could improve the model prediction accuracy. However, in the initial strat up period until about 95 seconds, the predicted mass flow rate was 6% larger than the experiment value. At the peak point at around 100 seconds, the expected value was smaller than that experiment value. The current Mean Relative Error (MRE) of this model for the entire period was 2%. In our study, we did not optimize the structure of the CNN-network. We also did not study which activation functions were the best in this case. Thus, there would still be some space for this model to be improved. Another drawback of this method was the 0-value shifting. As shown in Figure 4, in the first 80 seconds before the system startup, the predicted mass flow rate value was not exactly 0. The training time for building the model was 5 minute 44 seconds using one CPU, but after one-time training, the prediction work could be completed immediately.

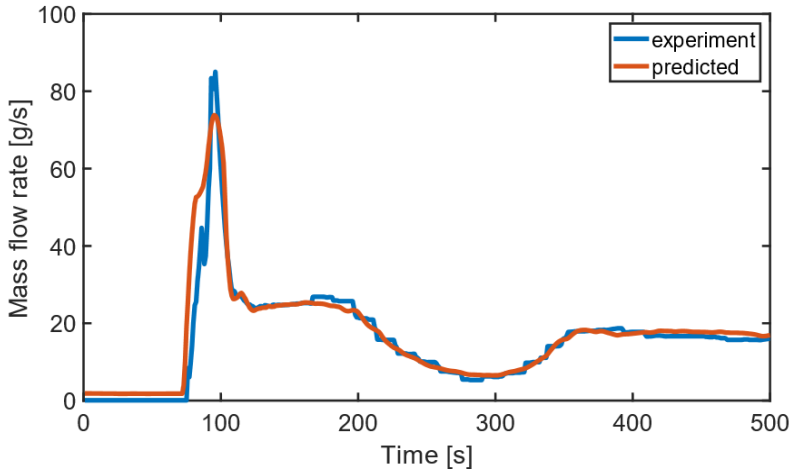

Figure 4: Mass Flow Rate Comparisons (CNN based model vs. Experiment)

4. CONCLUSIONS

A field test of VRF system was conducted in a campus office building. The start-up process of the target system was studied. The conclusions can be listed below:

- The pressure change and mass flow rate change had around a 100-second delay as compared with the control parameters like compressor frequency and EEV opening degree;
- For the system mass flow rate prediction, the compressor performance map failed to predict the first 100 seconds. A 20-second delay existed between the experiment value and the predicted value; and
- We introduced a CNN-based model to solve this problem. The CNN-based model could predict the transient data without delay. The current model's MRE is 2%. However, a 6% still exist at the peak point of the mass flow rate.

Future work can be how to make the current model more robust and reliable. Also, how to combine the strengths of the knowledge-based method and physics-based methods could be further studied. We also plan to develop a black-box model and a grey box model for the whole system. The black-box model can be a classification problem and used to detect different control logics.

NOMENCLATURE

COP	Coefficient of Performance
EEV	Electronic Expansion Valve
CNN	Convolutional Neural Network
VRF	Variable Refrigerant Flow
OU	Outdoor Unit
IU	Indoor Unit
ReLu	Rectified Linear Unit
MRE	Mean Relative Error
HPVRF	Heat Pump Variable Refrigerant Flow

REFERENCES

Goetzler, W., 2007. Variable refrigerant flow systems. Ashrae Journal 49, 24–31.

Kwon, L., Lee, H., Hwang, Y., Radermacher, R., Kim, B., 2014. Experimental investigation of multifunctional VRF system in heating and shoulder seasons. Applied Thermal Engineering 66, 355–364. https://doi.org/10.1016/j.applthermaleng.2014.02.032

Li, G., Hu, Y., Chen, H., Shen, L., Li, H., Li, J., Hu, W., 2016. Extending the virtual refrigerant charge sensor (VRC) for variable refrigerant flow (VRF) air conditioning system using data-based analysis methods. Applied Thermal Engineering 93, 908–919. https://doi.org/10.1016/j.applthermaleng.2015.10.050

Lin, X., Lee, H., Hwang, Y., Radermacher, R., Oh, S., 2014. Experimental investigation of multi-functional variable refrigerant flow system.

Liu, J., Hu, Y., Chen, H., Wang, J., Li, G., Hu, W., 2016. A refrigerant charge fault detection method for variable refrigerant flow (VRF) air-conditioning systems. Applied Thermal Engineering 107, 284–293. https://doi.org/10.1016/j.applthermaleng.2016.03.147

Liu, J., Li, G., Chen, H., Wang, J., Guo, Y., Li, J., 2017. A robust online refrigerant charge fault diagnosis strategy for VRF systems based on virtual sensor technique and PCA-EWMA method. Applied Thermal Engineering 119, 233–243. https://doi.org/10.1016/j.applthermaleng.2017.03.074

Nasrabadi, N.M., 2007. Pattern recognition and machine learning. Journal of electronic imaging 16, 049901.

Shi, S., Li, G., Chen, H., Liu, J., Hu, Y., Xing, L., Hu, W., 2017. Refrigerant charge fault diagnosis in the VRF system using Bayesian artificial neural network combined with ReliefF filter. Applied Thermal Engineering 112, 698–706. https://doi.org/10.1016/j.applthermaleng.2016.10.043

Sun, K., Li, G., Chen, H., Liu, J., Li, J., Hu, W., 2016. A novel efficient SVM-based fault diagnosis method for multi-split air conditioning system's refrigerant charge fault amount. Applied Thermal Engineering 108, 989–998. https://doi.org/10.1016/j.applthermaleng.2016.07.109

Thornton, B., Wagner, A., 2012. Variable Refrigerant Flow Systems 79.

Wan, H., Cao, T., Hwang, Y., Chang, S.-D., Yoon, Y.-J., 2020a. Machine-Learning-Based Compressor Models: A Case Study for Variable Refrigerant Flow Systems. International Journal of Refrigeration. https://doi.org/10.1016/j.ijrefrig.2020.12.003

Wan, H., Cao, T., Hwang, Y., Oh, S., 2020b. A review of recent advancements of variable refrigerant flow air-conditioning systems. Applied Thermal Engineering 169, 114893. https://doi.org/10.1016/j.applthermaleng.2019.114893

Wan, H., Cao, T., Hwang, Y., Oh, S., 2019. An Electronic Expansion Valve Modeling Framework Development Using Artificial Neural Network: A Case Study on VRF Systems. International Journal of Refrigeration S0140700719303676. https://doi.org/10.1016/j.ijrefrig.2019.08.018

Yu, F., Li, G., Chen, H., Guo, Y., Yuan, Y., Coulton, B., 2018. A VRF charge fault diagnosis method based on expert modification C5.0 decision tree. International Journal of Refrigeration 92, 106–112. https://doi.org/10.1016/j.ijrefrig.2018.05.034

ACKNOWLEDGEMENT

We gratefully acknowledge the support of the Center for Environmental Energy Engineering (CEEE) at the University of Maryland, and System Air Conditioning Laboratory at LG Electronics Inc.